

Magnetic properties of first-row element-doped ZnS semiconductors: A density functional theory investigation

Run Long and Niall J. English

The SEC Strategic Research Cluster and the Centre for Synthesis and Chemical Biology, Conway Institute of Biomolecular and Biomedical Research, School of Chemical and Bioprocess Engineering, University College Dublin, Belfield, Dublin 4, Ireland

(Received 21 May 2009; revised manuscript received 11 July 2009; published 22 September 2009)

Based on first-principles calculations, we have investigated the magnetic properties of the first-row element-doped ZnS semiconductors. Calculations reveal that Be, B, and C dopants can induce magnetism while N cannot lead to spin polarization in ZnS. A possible explanation has been rationalized from the elements' electronegativity and interaction between dopant and host atoms. The total magnetic moments are 2.00, 3.16, and $2.38\mu_B$ per $2 \times 2 \times 2$ supercell for Be, B, and C doping, respectively, and ferromagnetic coupling is generally observed in these cases. The ferromagnetism of Be-, B-, and C-doped ZnS can be explained by hole-mediated *s-p* or *p-p* interactions' coupling mechanisms. The clustering effect was found to be present in Be-, B-, and C-doped ZnS but the degree is more obvious in the former two cases than in the latter case. Analysis revealed that C-doped ZnS displays better potential ferromagnetic behavior than Be- and B-doped ZnS due to its semimetallic characteristics.

DOI: 10.1103/PhysRevB.80.115212

PACS number(s): 75.50.Pp

I. INTRODUCTION

Diluted magnetic semiconductors (DMSs) have attracted intense interest due to their potential applications in spintronics devices.¹ To date, most of the attention on DMSs has been focused on transition-metal (TM)-doped semiconductors, such as GaN and ZnO.²⁻⁴ Typically, the Curie temperatures of such systems are below room temperature, meaning that they are difficult to use in practice. Recently, room-temperature ferromagnetism was reported in TM-doped DMSs but it was difficult to avoid the presence of TM clustering or secondary phases.⁵ In addition, for group II-VI semiconductors, it is difficult to dope such materials effectively to realize *p*- or *n*-type devices due to their intrinsic band gaps. A possible way to overcome this drawback is to use nonmetal elements to substitute TM magnetic elements to dope such semiconductors. In fact, there are many studies which have reported that nonmetal elements induce magnetic behavior both experimentally and theoretically.⁶⁻¹³ It has been demonstrated that room-temperature ferromagnetism can be achieved in ZnO by doping with C.⁶ Subsequently, it has been reported that stable ferromagnetism is extant in C-doped CdS and C-doped ZnS.^{7,8} Other nonmetal elements, such as Be, B, and N, can also lead to ferromagnetism in AlN and ZnO, respectively.⁹ Therefore it is possible that such nonmetal elements could also induce ferromagnetic (FM) coupling in ZnS. However, only Fan *et al.*⁸ have reported the electronic structure and magnetic properties of C anion-doped ZnS; a detailed theoretical investigation and comparison of Be-, B-, and N-doped ZnS has not been reported to date, to the best of our knowledge.

In the present study, we have employed first-principles calculations to study the magnetism and electronic structure of X (Be, B, C, and N)-doped ZnS systematically. Calculations indicate that doping by Be, B, and C atoms in ZnS could induce ferromagnetic coupling in ZnS through hole-mediated interactions. The magnetic moments were 2.00, 3.16, and $2.38\mu_B$ for Be-, B-, and C-doped 64-atom ZnS

containing one substitutional dopant atom. However, the incorporation of the N dopant did not result in spin polarization in N-doped ZnS. Consideration of the elements' electronegativity and bonding characteristics can explain the different behavior in doped systems for B, Be, C, and N. The electronic structures show that Be doping of ZnS induces deep acceptor levels inside the band gap while B-doped ZnS is a *p*-type semiconductor and C-doped ZnS is a *p*-type semimetallic ferromagnetic semiconductor. *p-d* exchange-like *p-p* coupling (*s-p* coupling for Be-doped ZnS) was found to be responsible for the ferromagnetic behavior.

II. METHODOLOGY

The spin-polarized calculations were performed using the projector augmented wave pseudopotentials as implemented in the Vienna *ab initio* Simulation Package code.^{14,15} The Perdew and Wang parameterization¹⁶ of the generalized gradient approximation¹⁷ was adopted for the exchange-correlation potential. The electronic wave function was expanded in-plane waves up to a cutoff energy of 400 eV and a Monkhorst-Pack *k*-point mesh¹⁸ of $4 \times 4 \times 4$ was used for geometry optimization and electronic property calculations. Both the atomic positions and cell parameters were optimized until the residual forces were below 0.01 eV/Å. The ZnS was modeled by a $2 \times 2 \times 2$ 64-atom zinc-blende structure ZnS supercell and doped systems were constructed with one or two dopant atoms to substitute host S atoms. The optimized lattice parameter for pure ZnS was 5.446 Å, in good agreement with an experimental value of 5.41 Å,¹⁹ indicating that our methodology is reasonable.

III. RESULTS AND DISCUSSIONS

First, we show the structural and energy results for different doping systems. In this case, one dopant atom was substituted for an S atom in the 64-atom supercell (cf. Fig. 1, site 1); the calculated results are listed in Table I. After ge-

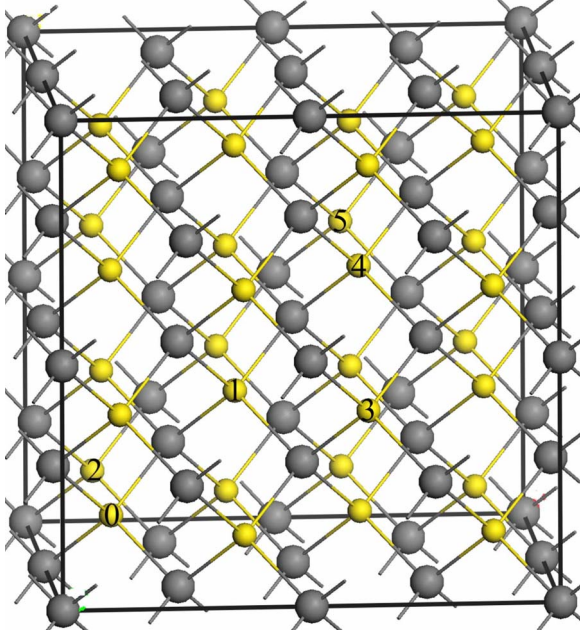


FIG. 1. (Color online) 64-atom ($2 \times 2 \times 2$) supercell of ZnS employed to define model Be, B, C, and N-doped ZnS structures. The small yellow and large gray spheres represent the S and Zn atoms, respectively. The positions of S substituted by dopant atoms are denoted by 0–5.

ometry relaxation, the relaxed X -Zn (X =Be, B, C, and N) bond length was 2.354, 2.209, 2.056, and 1.980 Å, respectively, which are all less than that of the optimal S-Zn bond length of 2.358 Å. The local structure around the dopant atoms was slightly suppressed with the Zn atoms close to the dopant atom.

To investigate the stability of doped ZnS, the defect formation energy E_{form} was calculated according to the following formula^{7,8,20}

$$E_{\text{form}} = E(\text{doped}) - E(\text{pure}) + n(\mu_{\text{S}} - \mu_{\text{X}}), \quad (1)$$

where $E(\text{doped})$ and $E(\text{pure})$ are the total energy of the ZnS supercell with and without the X dopants. μ_{X} is the chemical potential for the X dopants (X =Be, B, C, or N) and μ_{S} is the chemical potential for S host atom, which depends on the material growth conditions and satisfies boundary conditions. n is the number of S atoms replaced by X dopants. We em-

ployed the same method as Fan *et al.*⁸ to calculate the chemical potentials for host and dopant atoms (i.e., the energies of an isolated S, Be, B, C, and N atoms, respectively). The results are summarized in Table I. They show that the formation energies are 5.47, 2.69, 1.49, and 1.33 eV, respectively. The smaller the formation energy, the easier the dopants' incorporation into the ZnS lattice; this indicates that C- and N-doped ZnS may be realized easily experimentally. Our calculated formation energy was 1.49 eV, which is somewhat larger than 0.98 eV reported in previous work.⁸

Calculations show that Be-, B-, and C-doped ZnS materials favor spin-polarized (E_{sp}) states and their total energies are 187, 501, and 98 meV lower than those of nonspin-polarized (E_{nsp}) states ($\Delta E = E_{\text{nsp}} - E_{\text{sp}}$), respectively, as shown in Table I; this indicates that the spin-polarized state is stable. However, there is an equivalent total energy between spin-polarized and nonspin-polarized calculations, suggesting that N cannot lead to spin splitting in N-doped ZnS; this was confirmed by subsequent electronic structure results (*vide infra*).

The calculated magnetic moments were 2.00, 3.16, and $2.38\mu_{\text{B}}$ for Be-, B-, and C-doped ZnS supercells, respectively. However, as stated previously, N doping did not lead to magnetic behavior. For Be-doped ZnS, the total magnetic moment ($2.00\mu_{\text{B}}$) per supercell arises mainly from Be atoms ($0.57\mu_{\text{B}}$ per Be atom). Each nearest neighboring Zn atom contributed $0.23\mu_{\text{B}}$ and each second-nearest neighboring S atom contributed $0.044\mu_{\text{B}}$. For B-doped ZnS, the total magnetic moment ($3.16\mu_{\text{B}}/\text{B}$) per supercell is attributable mainly to the B atom itself ($1.01\mu_{\text{B}}/\text{B}$). Each nearest neighboring Zn atom provided $0.32\mu_{\text{B}}$ and each second-nearest S atom contributed $0.07\mu_{\text{B}}$. For C-doped ZnS, the total magnetic moment per supercell ($2.38\mu_{\text{B}}/\text{C}$) was due principally to C atoms ($0.70\mu_{\text{B}}/\text{C}$), which is slightly larger than $2.00\mu_{\text{B}}$ per supercell reported by Fan *et al.*⁸ in C-doped ZnS. Each nearest-neighboring Zn atom contributed $0.14\mu_{\text{B}}$ and each second-nearest-neighboring S atom contributed $0.082\mu_{\text{B}}$. It is well known that so many factors can influence the magnetic-moment value, such as the supercell volume, local structure, and so on. Certainly, the supercell volume is 1274 \AA^3 (with this value not specified in Ref. 8) and the difference in the Zn-C bond length between our results and those of Ref. 8 is 0.007 Å. These two factors may account for the difference of the total magnetic moment and local magnetic moment on the C atom between our work and that of Fan *et al.*⁸ In all of these doped systems, the magnetic

TABLE I. Optimized X -Zn (X =Be, B, C, and N) bond lengths. Total energy difference between spin-polarized (E_{sp}) and nonspin-polarized (E_{nsp}) states, $\Delta E = E_{\text{nsp}} - E_{\text{sp}}$. Formation energy (E_{form}) for the introduction of a dopant atom into the S site of ZnS based on the stable configuration. Magnetic moment of X ion M_{X} and total magnetization of the supercell, M_{tot} , in its stable state.

Models	X -Zn (Å)	ΔE (meV)	E_{form} (eV)	$M_{\text{X}}(\mu_{\text{B}})$	$M_{\text{tot}}(\mu_{\text{B}})$
Be@S	2.354	187	5.47	0.57	2.00
B@S	2.209	501	2.69	1.01	3.16
C@S	2.056	98	1.49	0.70	2.38
N@S	1.980	0	1.33	0	0

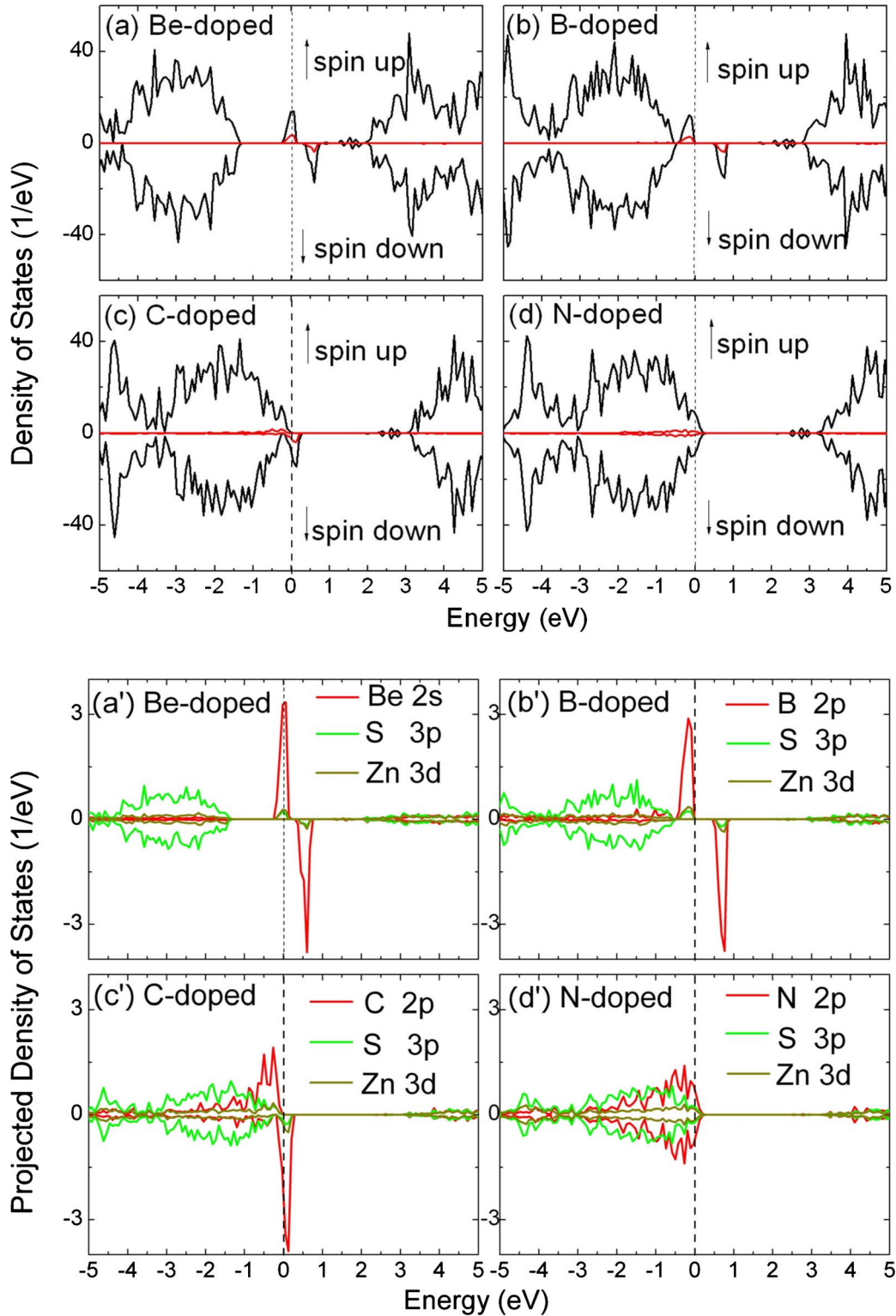


FIG. 2. (Color online) (a) DOS and (b) PDOS. Black, red, green, and dark yellow lines represent the total DOS, dopants 2p (2s orbital for Be), S 3p, and Zn 3d orbitals, respectively. The dashed line represents the Fermi level E_F .

moments are oriented in the same direction, indicating ferromagnetic coupling between the dopant (Be, B, and C) and neighboring host atoms.

Figure 2 shows the calculated total density of states (DOS) and the projected DOS (PDOS) of ZnS with one S atom substituted by dopant atoms (Be, B, C, and N) and one

of the neighboring S and Zn atoms. The interaction between the atomic orbitals and the conduction band (CB) or valence band (VB) leads to the formation of antibonding and bonding states. In the case of N as the dopant, these bonding and antibonding states will reside in the VB and CB, respectively. The electronegativities are in the order Be(1.57)

$<B(2.04) < C(2.55) < S(2.58) < N(3.04)$.²¹ Since Be, B, and C are less electronegative than N, they therefore tend to interact less with the host semiconductor. Therefore the bonding or antibonding states due to the interaction with the VB or CB cannot be pushed up or down into the CB or VB and therefore stay in the gap. As shown in Fig. 2, the $2s$ orbitals of Be, $2p$ orbitals of B, and C locate in the gap and are very small within the host CB and VB, indicating that they are bonded more weakly to Zn atoms than N and therefore their $2s$ or $2p$ orbitals are more localized. This leads to spin polarization of their $2s$ or $2p$ states, to reduce the Coulombic interaction energy and the total system energy to keep the system stable. On the other hand, N is more electronegative than S and interacts with the host atoms more strongly, which results in bonding and antibonding states giving a larger splitting while they still reside in the host bands. The above bond length also indicates that the interaction between dopant atoms and Zn atoms is in the order $Be-Zn < B-Zn < C-Zn < N-Zn$.

Figure 2 shows that Be, B, and C dopants change the DOS significantly near the Fermi level, E_F , and result in a significant spin polarization of the VB but does not induce spin polarization of the CB. Strong coupling between the s orbitals of Be, p orbitals of B, C, and S atoms and the d orbitals of Zn atoms near the Fermi level can be seen clearly. The d orbitals of Zn are hybridized with the s or p orbitals of the dopant and host S atom. The spin-up bands are fully occupied for B- and C-doped ZnS while the spin-down bands are empty, leading to a significant spin splitting. At the same time, the position of the Fermi level in B- and C-doped ZnS is different. In particular, E_F is between majority- and minority-spin states in B-doped ZnS and is in the VB tail in C-doped ZnS, indicating that the former system constitutes a good p -type ferromagnetic semiconductor and the latter case a p -type semimetallic ferromagnetic semiconductor. This suggests that for these two cases, the charge carriers within the impurity bands are sufficiently mobile, which is not only beneficial for conductive behavior but also for magnetic coupling. Furthermore, the semimetallic character of C-doped ZnS can complete spin polarization (100%) at the Fermi level, which is important for spintronics applications.²² On the other hand, E_F was pinned to the impurity states in the band gap of Be-doped ZnS, which implies that the extent of electronic localization is high and that electrons cannot move

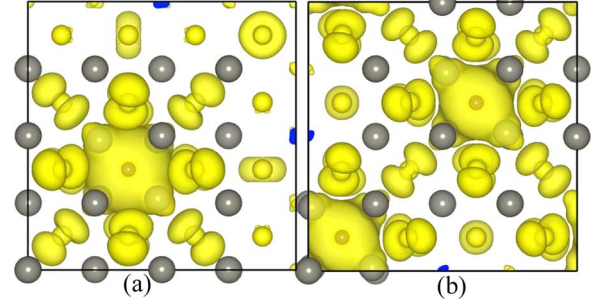


FIG. 3. (Color online) Spin density for (a) single-C doping (left panel) and (b) two-C doping (right hand) for a FM state separated by 7.638 Å. The yellow isosurface corresponds to the spin-up density.

freely. Hence, Be-doped ZnS possesses weak conductive behavior and does not facilitate magnetic interaction.

Based on the above analysis, we have selected C-doped ZnS as an example for analysis of its spin-density distribution. This is shown in Fig. 3(a), where the spin density in C-doped ZnS is localized mainly on the C atom and distributed slightly over its four nearest-neighboring Zn atoms and the 12 second-nearest-neighboring S atoms. This indicates that magnetic orbital coupling extends to the second-nearest-neighboring S atoms from the C dopant centers. Therefore, anions from the delocalized p orbitals contribute chiefly to the magnetic moment in C-doped ZnS.

To investigate the magnetic order, we investigated two dopant atoms substituted for two S atoms in the ZnS host semiconductor. Five possible and independent configurations of the two dopant atoms were considered, i.e., $Be(B,C)_{0i}$ ($i=1-5$), as shown in Fig. 1. In each case, one dopant atom occupied position 0 and the other dopant atom was located at other host S atom positions (1–5). The energy difference between FM and antiferromagnetic (AFM) states [$\Delta E = E(\text{FM}) - E(\text{AFM})$] for three doped configurations are summarized in Tables II–IV. Calculations indicated that there exists a FM state in Be-, B-, and C-doped ZnS semiconductors, suggesting that long-range ferromagnetic coupling exists between the three kinds of dopant atoms. Such large energy differences between FM and AFM states for the three doped FM systems [380, 751, and 121 meV in (0, 5), (0, 5) and (0, 4) configurations for Be, B and C doping, respectively] suggest that room-temperature ferromagnetism for

TABLE II. Be-doped ZnS. Energy difference between FM and AFM spin ordering $\Delta E = E(\text{FM}) - E(\text{AFM})$. Formation energy (E_{form}) for the introduction of two dopant atoms into the S sites of ZnS based on the stable configuration (FM or AFM). Absolute value of magnetic moment on each Be ion M_{Be} and total magnetization of the supercell, M_{tot} , in its stable state (FM or AFM) for different Be-Be distances in the doping configurations shown in Fig. 1, i.e., $Be(0, i)$ ($i=1-5$).

(0, i)	Be-Be (Å)	ΔE (meV)	E_{form}	$M_{\text{Be}}(\mu_B)$	$M_{\text{tot}}(\mu_B)$
(0, 1)	3.819	18	9.00	0.20	0
(0, 2)	5.401	-212	10.71	0.57	4.10
(0, 3)	6.615	94	10.52	0.56	0
(0, 4)	7.638	3	10.27	0.001	0
(0, 5)	9.355	-380	10.87	0.58	3.98

TABLE III. B-doped ZnS. Energy difference between FM and AFM spin ordering $\Delta E = E(\text{FM}) - E(\text{AFM})$. Formation energy (E_{form}) for the introduction of two dopant atoms into the S sites of ZnS based on the stable configuration (FM or AFM). Absolute value of magnetic moment on each B ion M_{B} , and total magnetization of the supercell, M_{tot} , in its stable state (FM or AFM) for different B-B distances in the doping configurations shown in Fig. 1, i.e., B(0, i) ($i=1-5$).

(0, i)	B-B (Å)	ΔE (meV)	E_{form}	$M_{\text{B}}(\mu_{\text{B}})$	$M_{\text{tot}}(\mu_{\text{B}})$
(0, 1)	3.819	9	4.81	0.74	0
(0, 2)	5.401	-10	5.36	1.00	6.36
(0, 3)	6.616	87	5.30	0.97	0
(0, 4)	7.638	-77	5.48	1.00	6.27
(0, 5)	9.355	-751	5.38	1.01	6.30

Be-, B-, and C-doped ZnS is quite feasible. However, C-doped ZnS in different configurations are not always in the FM state in our calculations, which contrasts with Fan *et al.*⁸ who reported that the FM state is always in the ground state. Our energy results indicate that the existence or stability of FM, AFM, and paraferromagnetic behavior may depend on the distance between two C dopant atoms. The same effect was observed in Be-doped ZnS. However, the nearest distance for the (0, 1) case of two dopant atoms exhibits the lowest formation energies and is over 1 and 0.57 eV lower than others in Be- and B-doped ZnS, respectively, indicating a clustering effect of Be and B. On the other hand, the formation energies of the (0, 1) AFM configuration is only about 0.08 eV lower than the FM (0, 4) configuration in C-doped ZnS, indicating that the clustering effect is not obvious. This would suggest that C-doped ZnS displays the best potential ferromagnetic behavior among the three doped systems.

At this point, it is instructive to investigate the magnetic coupling between the two dopant atoms. Magnetic coupling was found to exist even if the separation distance was 9.355 Å for Be- and B-doped ZnS [the (0, 5) configuration] and by 7.638 Å for C-doped ZnS [the (0, 4) case]. However, both double-exchange and superexchange interactions cannot account for long-range magnetic order at low doping concentrations of a few percent. The double exchange occurs due to electron exchange via unoccupied bands or impurity-related bands of two adjacent dopants without spin reversal.^{23,24} The

electron clouds should at least overlap each other. In our case, the distance between two dopants is very large and the doping concentrations are very low at the same time. This suggests that double exchange is not responsible for long-range FM coupling. In addition, although double exchange via empty states in the conduction band may also be a factor, this contribution is small in zinc-blende host crystals because the hybridization between the impurity d and s states of the electrons near the bottom of conduction band is weak due to symmetry selection rules.^{25,26} Hence, it is possible that p - d exchange-like p - p coupling (s - p coupling for Be-doped ZnS) involving holes are responsible for the observed long-range magnetic coupling similar to N-doped ZnO.¹⁰ For conciseness, we have selected C-doped ZnS as a representative system to discuss long-range magnetic coupling. Figure 3(b) shows magnetic coupling between two C atoms. As can be seen, the nearest-neighbor anions between dopants mediate the magnetic coupling. Obviously, the charge carriers localized around the anions between the C atoms are polarized and the spin orientations are parallel to each other. Consequently, these polarized charge carriers mediate the long-range ferromagnetic coupling between the dopant atoms. There are four valence electrons in a C ion, which has two less valence electrons than an S ion. Replacement of S by C introduces more holes into the valence band. Hole-mediated ferromagnetism may be responsible for magnetic coupling. The strong p - p interaction leads to a stronger coupling between impurity and carrier spin orientations. Sufficiently

TABLE IV. C-doped ZnS. Energy difference between FM and AFM spin ordering $\Delta E = E(\text{FM}) - E(\text{AFM})$. Formation energy (E_{form}) for the introduction of two dopant atoms into the S sites of ZnS based on the stable configuration (FM or AFM). Absolute value of magnetic moment on each C ion M_{C} and total magnetization of the supercell, M_{tot} , in its stable state (FM or AFM) for different C-C distances in the doping configurations shown in Fig. 1, i.e., C(0, i) ($i=1-5$).

(0, i)	C-C (Å)	ΔE (meV)	E_{form}	$M_{\text{C}}(\mu_{\text{B}})$	$M_{\text{tot}}(\mu_{\text{B}})$
(0, 1)	3.819	56	2.59	0.51	0
(0, 2)	5.401	4	2.90	0.71	0
(0, 3)	6.616	-59	2.68	0.83	4.63
(0, 4)	7.638	-121	2.67	0.67	3.83
(0, 5)	9.355	0	2.81	0	0

large spin-polarized carriers are able to effectively mediate indirect long-range ferromagnetic coupling between the C dopants, as shown in Fig. 3(b). The spatially extended p states of the host and the impurity are able to extend the p - p interaction and spin alignment to longer range, and thus to cause long-range magnetic coupling between the impurities. Similar analysis may be applied to Be- and B-doped ZnS.

IV. CONCLUSIONS

We have studied Be, B, C, and N anion-doped ZnS by means of density functional theory calculations. It has been shown that Be, B, and C impurities acquire magnetization, leading to a magnetic moment of 2.00, 3.16, and $2.38\mu_B$ per $2 \times 2 \times 2$ supercell while N-doped ZnS displays no magnetic behavior. The lower Be, B, and C electronegativities vis-à-vis S lead to weaker interactions between dopants and host atoms, and serve to keep the dopants' $2s$ or $2p$ states within the band gap. Conversely, the larger N electronegativity in comparison to S leads to a stronger interaction between N

and host atoms which results in the $2p$ states residing in the host bands. The magnetic moments of Be, B, and C and its neighboring Zn and S atoms are parallel. Based on the calculated results that impurity bands are located within the band gap and the Fermi level crosses the impurities, long-range ferromagnetic coupling between two dopant atoms has been attributed to hole-mediated p - p coupling (s - p coupling for Be-doped ZnS) interactions. The clustering effect was found in three doped systems although it is not obviously apparent in C-doped ZnS. Considering its lower formation energy, room-temperature ferromagnetism and semimetallic characteristics, C-doped ZnS may be more readily achievable in comparison to Be- and B-doped ZnS.

ACKNOWLEDGMENTS

This work was supported by the Irish Research Council for Science, Engineering and Technology (IRCSET). The authors thank the Irish Centre for High End Computing and Science Foundation Ireland for the provision of computational resources.

-
- ¹H. Ohno, *Science* **281**, 951 (1998).
²C. Liu, F. Yun, and H. Morko, *J. Mater. Sci. Mater. Electron.* **16**, 555 (2005).
³H. Munekata, H. Ohno, S. von Molnar, Armin Segmüller, L. L. Chang, and L. Esaki, *Phys. Rev. Lett.* **63**, 1849 (1989).
⁴M. H. F. Sluiter, Y. Kawazoe, P. Sharma, A. Inoue, A. R. Raju, C. Rout, and U. V. Waghmare, *Phys. Rev. Lett.* **94**, 187204 (2005).
⁵S. Zhou, K. Potzger, J. von Borany, R. Grötzschel, W. Skorupa, M. Helm, and J. Fassbender, *Phys. Rev. B* **77**, 035209 (2008).
⁶H. Pan, J. B. Yi, L. Shen, R. Q. Wu, J. H. Yang, J. Y. Lin, Y. P. Feng, J. Ding, L. H. Van, and J. H. Yin, *Phys. Rev. Lett.* **99**, 127201 (2007).
⁷H. Pan, Y. P. Feng, Q. Y. Wu, Z. G. Huang, and J. Lin, *Phys. Rev. B* **77**, 125211 (2008).
⁸S. W. Fan, K. L. Yao, and Z. L. Liu, *Appl. Phys. Lett.* **94**, 152506 (2009).
⁹X. Y. Peng and R. Ahujia, *Appl. Phys. Lett.* **94**, 102504 (2009).
¹⁰L. Shen, R. Q. Wu, H. Pan, G. W. Peng, M. Yang, Z. D. Sha, and Y. P. Feng, *Phys. Rev. B* **78**, 073306 (2008).
¹¹B. Gu, N. Bulut, T. Ziman, and S. Maekawa, *Phys. Rev. B* **79**, 024407 (2009).
¹²I. R. Shein, A. N. Enyashin, and A. L. Ivanovskii, *Phys. Rev. B* **75**, 245404 (2007).
¹³K. S. Yang, Y. Dai, B. B. Huang, and M.-H. Whangbo, *Appl. Phys. Lett.* **93**, 132507 (2008).
¹⁴G. Kresse and J. Hafner, *Phys. Rev. B* **47**, 558 (1993).
¹⁵G. Kresse and J. Furthmüller, *Phys. Rev. B* **54**, 11169 (1996).
¹⁶J. P. Perdew, K. Burke, and M. Ernzerhof, *Phys. Rev. Lett.* **77**, 3865 (1996).
¹⁷J. P. Perdew and Y. Wang, *Phys. Rev. B* **45**, 13244 (1992).
¹⁸H. J. Monkhorst and J. D. Pack, *Phys. Rev. B* **13**, 5188 (1976).
¹⁹N. K. Abrikosov, V. B. Bankina, L. V. Poretskaya, L. E. Shelimova, and E. V. Skudnova, *Semiconducting II-VI, IV-IV and V-VI Compounds* (Plenum, New York, 1969).
²⁰S. B. Zhang and John E. Northrup, *Phys. Rev. Lett.* **67**, 2339 (1991).
²¹D. R. Lide, *CRC Handbook of Chemistry and Physics*, 87th ed. (Taylor & Francis, London, 2006).
²²S. A. Wolf, D. D. Awschalom, R. A. Buhrman, J. M. Daughton, S. von Molnar, M. L. Roukes, A. Y. Chtchelkanova, and D. M. Treger, *Science* **294**, 1488 (2001).
²³C. Zener, *Phys. Rev.* **82**, 403 (1951).
²⁴P.-G. de Gennes, *Phys. Rev.* **118**, 141 (1960).
²⁵K. A. Kiloin and V. N. Fleurov, *Transition Metal Impurities in Semiconductors* (World Scientific, Singapore, 1994).
²⁶A. Zunger, in *Solid State Physics*, edited by H. Ehrenreich and D. Turnbull (Academic, Orlando, 1986), Vol. 39, p. 276.